Anthropogenic perturbations of the silicon cycle at the global scale: the key role of the land-ocean transition

G. G. Laruelle[1], V. Roubeix[2], A. Sferratore[3], B. Brodherr[4], D. Ciuffa[5], D. J. Conley[6], H. H. Dürr[2,7], J. Garnier[3], C. Lancelot[2], Q. Le Thi Phuong[3], J.-D. Meunier[8], M. Meybeck[3], P. Michalopoulos[9], B. Moriceau[10], S. Ní Longphuirt[10], S. Loucaides[1], L. Papush[11], M. Presti[9], O. Ragueneau[10], P. A. G. Regnier[1,12], L. Saccone[13], C. P. Slomp[1], C. Spiteri[1], P. Van Cappellen[1]

[1] Department of Earth Sciences, Utrecht University, The Netherlands.
[2] Aquatic Systems Ecology, Université Libre de Bruxelles, Belgium.
[3] UMR 7619 Sisyphe, Université Pierre et Marie Curie, Paris, France.
[4] Department of Marine Biology, Baltic Sea Research Institute, Warnemünde, Germany.
[5] Centre for Research and Monitoring of the Marine Environment, University of Rome Tor Vergata, Italy.
[6] GeoBiosphere Science Centre, Department of Geology, Lund University, Sweden
[7] Department of Physical Geography, Utrecht University, The Netherlands.
[8] CEREGE, CNRS/Université Paul Cezanne, Aix en Provence, France.
[9] Hellenic Center for Marine Research, Athens, Greece.
[10] European Institute for Marine Studies, University of Western Brittany, Plouzané, France.
[11] Department of Water and Environment Studies, Linköping University, Sweden.
[12] Department of Earth and Environmental Sciences, Université Libre de Bruxelles, Belgium
[13] National Environmental Research Institute, Denmark

Corresponding author: G. G. Laruelle, g.laruelle@geo.uu.nl

FOR SUBMISSION TO

Global Biogeochemical Cycles

June 2009

Abstract

Silicon (Si), in the form of dissolved silicate (DSi), is a key nutrient in marine and continental ecosystems. DSi is taken up by organisms to produce structural elements (e.g., shells and phytoliths) composed of amorphous biogenic silica ($bSiO_2$). A global mass balance model of the biologically active part of the modern Si cycle is derived based on a systematic review of existing data regarding terrestrial and oceanic production fluxes, reservoir sizes, and residence times for DSi and $bSiO_2$. The model demonstrates the high sensitivity of biogeochemical Si cycling in the coastal zone to anthropogenic pressures, such as river damming and global temperature rise. As a result, further significant changes in the production and recycling of $bSiO_2$ in the coastal zone are to be expected over the course of this century.

1. Introduction

Silicon (Si) is the second most abundant element in the Earth's crust after oxygen. Most Si, however, is bound in the form of quartz and silicate minerals, and is therefore unavailable for uptake by organisms. Thus, despite its abundance, Si is a major limiting element in many aquatic systems (Conley and Malone, 1992; Egge and Aksnes, 1992; Paasche, 1980; Leynaert et al., 2001), and is also an essential nutrient for the growth of many terrestrial plants (Epstein, 1999; Datnoff et al., 2001). Key aspects of the global biogeochemical silicon cycle remain poorly understood, such as the biological cycling of Si on the continents (Conley, 2002a), the role of the coastal zones in regulating the transfer of reactive Si from land to the open ocean (Conley, 1997; DeMaster, 2002), the fate of biogenic silica produced in oceanic surface waters and its decoupling from carbon during sinking (Nelson et al., 1995; Ragueneau et al., 2002, 2006a), and ongoing changes to the Si cycle by human activities (Chauvaud et al., 2000; Conley et al., 1993; Friedl and Wuest, 2002; Friedl et al., 2004; Humborg et al., 2000, 2006; Ragueneau et al., 2005, 2006b, 2006c, Conley et al., 2008).

Global scale studies of the biogeochemical Si cycle have focused mainly on the marine aspect. An important landmark in the assessment of Si fluxes in the world ocean is the work of Tréguer et al. (1995). These authors, however, provide no estimates of the amounts of biogenic silica stored in the oceans and underlying sediments. Furthermore, only a crude representation of the land-ocean interface is included in their global Si budget. In this respect, the current state of knowledge and modeling of global carbon, nitrogen, phosphorus and sulfur cycles (Mackenzie et al., 1993, 1998; Ver, 1998; Rabouille et al., 2001) are significantly more advanced than for silicon.

In this study, we provide global scale estimates of reservoir sizes and fluxes of reactive Si on the continents in the ocean and at the continent-to-ocean transition. Emphasis is placed on the biogeochemical dynamics of Si at the Earth's surface, from the recent past to the end of the 21st century. We therefore do not explicitly represent the long-term endogenic Si cycling, but rather include the Earth's lithosphere as the ultimate source and sink of reactive Si. The two forms of reactive Si considered are dissolved silicate (DSi) and biogenic silica ($bSiO_2$). The main transformation processes in the global biogeochemical Si cycle are uptake of DSi followed by biomineralization as $bSiO_2$ in terrestrial plants and aquatic organisms, and the dissolution of $bSiO_2$ into DSi.

The resulting mass balance model is used to explore the sensitivity of the global Si cycle and gain insight into its function. Special attention is paid to the role of the coastal zone and continental shelves on the coupling of terrestrial and oceanic Si dynamics. In addition, the response of the global biogeochemical Si cycle to two anthropogenically-driven forcings is analyzed: global temperature rise and river damming. These forcings are selected because both siliceous production and $bSiO_2$ dissolution are sensitive to temperature (Wollast 1974; Cossins and Bowler, 1987; Rickert, 2000; Van Cappellen et al., 2002), while increased river damming, especially since the 1950's, has considerably modified the reactive Si delivery to the oceans (Conley, 2002b, Humborg et al., 2006).

2. Global biogeochemical Si model

2.1 Water cycle

The Earth's surface environment is divided into four compartments (Figure 1): continents (box 1), proximal (box 2) and distal (box 3) coastal zones, and the open ocean (box 4). The proximal and distal coastal zones are those proposed by Rabouille et al. (2001). As shown by these authors, this division of the global coastal zone provides a more realistic

representation of the role of continent to ocean transition in the biogeochemical cycling of carbon and nutrients. The proximal zone consists of large bays, the open water parts of estuaries, inner deltas, inland seas and coastal marshes (Woodwell et al., 1973). The distal zone comprises the rest of the continental margins up to the shelf break.

These compartments are linked to one another via the water cycle (Figure 1). Water on the continents is subdivided into an aquatic reservoir, which comprises exorheic rivers and lakes including their floodplains (Box 1a), and a groundwater reservoir (Box 1b). The open ocean is by far the largest compartment, with a mean water depth of 3600 m and covering 92% of the world ocean (Tréguer et al., 1995). Three vertical subcompartments of the water column are considered: a 100 m thick surface layer where photosynthesis takes place (Box 4a), mesopelagic oceanic waters (100-1000 m depth) (Box 4b) and deep waters (Box 4c).

Water fluxes (W) considered in the baseline scenario are based on the simplified steady-state water cycle summarized in Table 1. It should be noted that a contribution from subsurface groundwater discharge to the proximal coastal zone is explicitly considered ($W_{1b\text{-}2}$, Slomp and Van Cappellen, 2004). The combination of water reservoir sizes with water fluxes yields water residence times that agree well with previous studies (Garrels and Mackenzie, 1971; Broecker and Peng, 1982; Macdonald, 1998).

2.2 Reactive Si reservoirs

The DSi and $bSiO_2$ reservoir masses are time-dependent variables of the Si cycle model (Figure 2). DSi mainly consists of undissociated monomeric silicic acid, $Si(OH)_4$, and represents the main form under which silicon can be assimilated by organisms (Del Amo and Brzezinski, 1999). Organisms use DSi to build structural elements made of amorphous, hydrated silica, part of which is preserved after the death of the organisms (Simpson and Volcani, 1981; Conley and Schelske, 2001). Here, $bSiO_2$ includes the amorphous silica in

both living biomass and biogenic detritus in open waters, soils and sediments. It should be noted that $bSiO_2$ may undergo significant chemical and mineralogical changes (Van Cappellen et al., 2002), even including a complete diagenetic transformation of the opaline silica into alumino-silicate minerals (Michalopoulos et al., 2000).

In marine environments, the major producers of $bSiO_2$ are diatoms, although other organisms, such as radiolarians, sponges, and chrysophytes, may locally be important sources of $bSiO_2$ (Simpson and Volcani, 1981). On land, large quantities of DSi are fixed by higher plants and deposited as amorphous silica in so-called phytoliths (Piperno, 1988). The significant contribution of phytolith production and dissolution in the global Si cycle has only recently been highlighted (Bartoli, 1983; Meunier et al., 1999; Conley, 2002a).

Estimations of DSi and $bSiO_2$ reservoir sizes in the four earth surface compartments are summarized in Table 2. Reservoir masses are mostly derived from estimates of the average DSi or $bSiO_2$ concentrations and the volumes of the corresponding reservoirs. In some cases, however, the reservoir mass is calculated from flux estimates, assuming steady-state conditions. For example, the mass of DSi in the water column of the distal coastal ocean (72 Tmol Si) is obtained from the export flux of DSi and the water flux to the open ocean (Table 2). This estimate, combined with the reservoir volume (3600 Tm^3, Figure 1), then yields an average DSi concentration of the distal ocean of 20 µM, which can be compared to the wide range of observed, depth-integrated DSi concentrations in shelf waters from <5µM (Alvarez-Salgado et al., 1997; Gibson et al., 1997, Lacroix et al., 2007) to ~ 15µM (Heiskanen and Keck, 1996) to >30µM, (Serebrennikova and Fanning, 2004; Zhang, 2002).

The ultimate source of DSi for the global Si cycle is chemical weathering of silicate rocks of the continental and oceanic crust (Gerard and Ranger, 2002). The total mass of silicate rock exposed at the Earth's surface largely exceeds that of the reactive DSi plus $bSiO_2$ reservoirs. Thus, on the time scales investigated (years to centuries), the reservoir size of

silicate rocks remains essentially unchanged. A large fraction of DSi released by weathering is converted by plants into phytoliths and temporarily stored in soils (Saccone et al., 2008; Figure 2). A rough estimate of the reservoir mass of $bSiO_2$ in soils is obtained based on average phytolith concentrations for different types of soils (Conley et al., 2002b), the average soil $bSiO_2$ concentration, and the global volume of soils. The latter is derived from the FAO world soil map (FAO/UNESCO, 1986), assuming a mean soil depth of 1 meter (Pouba, 1968; Batjes, 1997).

The sediment reservoirs correspond to the topmost layers where decomposition of biogenic constituents drives the return of dissolved nutrient species to the water column (including DSi). The corresponding volumes (VS, Table 2) are estimated by assigning a mean thickness of 10 cm to the active layer of aquatic sediments on the continents and in the proximal coastal zone (Heinze et al., 1999), and 20 cm for distal coastal zone and deep sea sediments (De Master, 2002). An average porosity of 0.7 and an average dry density of 2.5 g cm^{-3} are assumed for all sediments (Maher et al., 2004). The calculated sediment volumes of boxes 1, 2, 3 and 4 are 1.73, 0.18, 5.5 and 75 Tm^3, respectively.

2.3 Reactive Si fluxes

The fluxes of reactive Si are obtained from the literature, or constrained by assuming that the Si cycle is initially at steady-state (Table 3). The assumption of an initial steady-state is a common practice in the modeling and budgeting of global elemental cycles (e.g., Mackenzie et al., 1993; Tréguer et al., 1995; Yool and Tyrrell, 2003). It is most likely that, given the oceanic residence time of reactive Si is 15000-17000 years (Tréguer et al., 1995), the marine Si cycle was not at steady state prior to 1950, due to glacial-interglacial changes. Nonetheless, considering the time scales investigated in the simulations ($\leq$ 150 years), these

much longer term changes have little effect on the system's response to the imposed perturbations.

The fluxes include the sources and sinks of reactive Si for the Earth's surface environment (Figure 2). The sources are chemical weathering on land (F_w) and flux of DSi to the oceans resulting from basalt-seawater interactions (F_{hyd}). The sinks are burial of $bSiO_2$ in sediments ($F_{C5\text{-}burial}$, $F_{P4\text{-}burial}$, $F_{S4\text{-}burial}$, $F_{O8\text{-}burial}$), and removal of DSi due to reverse weathering reactions in shelf sediments (F_{S3rw}, Mackenzie and Garrels, 1966; Michalopoulos and Aller, 1995, 2004). Note that, because we assume an initially steady-state Si cycle, the sinks and sources of reactive Si balance each other exactly.

All other fluxes either transform or transport reactive Si within the Earth's surface environment and are thus internal fluxes. Si fluxes are represented by the symbol "F" followed by a subscript that identifies the initial (source) and final (sink) reservoir. The reservoir symbols are listed in Tables 1 and 2, for water and reactive Si reservoirs, respectively. Fluxes describing the uptake of DSi by organisms to produce $bSiO_2$ (F_{C1C2}, F_{C3C4}, F_{P1P2}, F_{S1S2}, F_{O1O2}) scale to the primary production rates in the various compartments of the earth surface environment (Table 3). Most $bSiO_2$ is efficiently recycled via dissolution in the water column (F_{C4C3}, F_{P2P1}, F_{S2S1}, F_{O2O1}, F_{O4O3}, F_{O6O5}), soils (F_{C2C1}) and sediments (F_{C5C3}, F_{P4P3}, F_{S4S3}, F_{O8O7}). The accumulation of DSi in the pore waters of sediments and progressive loss in the reactivity of biogenic silica surfaces (ageing) ultimately allows a small fraction of $bSiO_2$ production to be buried and preserved in sediments (Van Cappellen et al., 2002).

The groundwater discharge flux of DSi to the coastal zone (F_{C1P1}) is derived from the corresponding water flux ($W_{1a\text{-}2}$ in Figure 1) and the average DSi concentration in groundwater. The riverine supply of DSi to the proximal zone (F_{C3P1}) is derived by averaging the estimated river DSi delivery fluxes computed for 150 coastal segments in the GEMS-GLORI (Meybeck and Ragu, 1995) and GEMS-PRISRI (Meybeck et al., 2003) databases,

under pristine conditions, that is, prior to human perturbation (Dürr et al., submitted). The estimated river DSi flux (6.2 Tmol y^{-1}) thus implicitly corrects for the drop in DSi concentration in the downstream reaches of rivers that has accompanied the extensive building of dams since the 1950s (Humborg et al., 2006). Note that, while the main source of reactive Si for the oceans is in the form of DSi, the contribution of riverine $bSiO_2$ delivery (F_{C4P2}) is far from negligible (Conley et al., 2000). Reactive Si is also supplied to the oceans via the atmosphere with eolian dust (F_{C2O2}), although this flux is most likely very small (Tréguer et al. 1995) and its origin (biogenic vs. mineral) remains poorly know (Cole et al., 2009; Dürr et al., submitted).

Transport fluxes of DSi into the ocean (F_{P1S1}, F_{S1O1}, F_{O3S1}, F_{O3O1}, F_{O5O3}), as well as export fluxes of $bSiO_2$ from the proximal zone to the distal zone (F_{P2S2}) and from the distal zone to the open ocean (F_{S2O2}), are assumed to be directly coupled to the water cycle. That is, the flux of DSi or $bSiO_2$ exiting the reservoir is related to the mass of DSi or $bSiO_2$ in that reservoir according to:

$$\frac{F_{ij}}{S_i} = \frac{Q_{ij}}{V_i} \quad (1)$$

where F_{ij} and Q_{ij} are, respectively, the fluxes of reactive Si and water from reservoir *i* to reservoir *j*, S_i is the mass of DSi or $bSiO_2$ in reservoir *i*, and V_i is the volume of the reservoir.

The remaining transport fluxes correspond to sedimentation (F_{O2O4}, F_{O4O6}) and deposition of $bSiO_2$ (F_{C4C5}, F_{P2P4}, F_{S2S4}, F_{O6O8}), and the efflux of DSi from sediments (F_{C5C3}, F_{P3P1}, F_{S3S1}, F_{O7O6}). In the marine realm, these fluxes are relatively well constrained by observations. Sedimentation rates and DSi fluxes from sediments can be determined directly with sediment traps and benthic chambers, respectively (Koning et al., 1997; Rao and Jahnke, 2004). Furthermore, numerous estimates of benthic DSi efflux have been calculated from measured pore water profiles (Rabouille et al., 1993; Dixit and Van Cappellen, 2003).

A widely used approach in biogeochemical box modeling is to relate the reservoir sizes and fluxes via linear expressions,

$$F_{ij} = k_{ij} S_i \quad (2)$$

where k_{ij} is a first order rate constant (Lasaga, 1981; Chameides and Perdue, 1997; Mackenzie et al., 1998). Values of k_{ij} range from values of 1 y^{-1}, for example for biological DSi uptake and $bSiO_2$ dissolution in aquatic environments, to values of 10^{-3} y^{-1} or less for groundwater transport of DSi or burial of $bSiO_2$ in the deep-sea sediments.

2.4 Model simulations

The mass balance equations for the various reactive Si reservoirs, based on the linear flux equations (2), are solved in MATLAB using Euler's method. The steady-state silica cycle represented in Figure 2 is taken as the initial condition. After verifying that the state variables exhibit no drift under time-invariant conditions, a time-dependent change in forcing is imposed, as detailed below. The system behavior is monitored for a period of 150 years, using an integration time step of 0.01 y. The starting time of the imposed perturbations is nominally set to 1950.

To simulate the response of the Si cycle to a global temperature increase, three different time-courses for mean surface air temperature are considered (low, medium and high; Figure 3), based on projections of the Intergovernmental Panel on Climate Change (IPCC, 1995). The three scenarios diverge after the year 2000. For simplicity, linear functions are used to describe the rising air-temperature. Temperatures of surface waters (Box 1a, Box 2, Box 3 and Box 4a) are assumed to follow air temperature, while the magnitude of the temperature rise of the intermediate oceanic waters is four times lower (Levitus, 2000). The initial temperature of the intermediate water is set to 5°C (Yool and Tyrell, 2003).

The processes that are directly affected by temperature in the simulations are biological DSi uptake, $bSiO_2$ dissolution and chemical weathering. The model assumes that, at the spatial and temporal scales resolved, an increase (decrease) in siliceous phytoplankton production results in an increase (decrease) in DSi fixation. In particular, we assume that a temperature-dependent change in primary production by diatoms causes a proportional change in DSi uptake. The temperature dependence of DSi uptake in continental and marine environments is described by the Eppley function ($\text{uptake rate} \propto e^{(0.07 \bullet T)}$, where T is temperature in °C, Eppley, 1972). This exponential function is widely used to describe the response of planktonic communities to temperature variations, except under extreme temperature conditions (Pasquer et al., 2005). This formulation implies the assumption that changes in DSi uptake linearly follow diatom growth. In the absence of relationships specifically describing the temperature dependence of DSi uptake by higher plants on land, we opt for a simple Q_{10} function, whereby the uptake rate doubles with every 10°C temperature increase (Winkler et al., 1996). The Arrhenius equation is used to correct the rates of $bSiO_2$ dissolution and silicate weathering (Lasaga, 1998). Reported activation energies for the dissolution of framework silicates and $bSiO_2$ fall mostly in the range 25-90 kJ mol^{-1} (Blum and Stillings, 1995; Van Cappellen et al., 2002). Here, a single Arrhenius activation energy of 60 kJ mol^{-1} is imposed, to account for the effect of temperature changes on both silicate rock weathering and $bSiO_2$ dissolution.

Another major effect of human activity on the cycling of reactive Si at the Earth's surface is the construction of dams, known to trap large quantities of $bSiO_2$ (Conley et al., 2000; Humborg et al., 2006). To test the sensitivity to damming, a correction coefficient is added to the flux equation describing $bSiO_2$ accumulation in sediments on the continents (F_{C4C5}). This coefficient is assigned a value of 1 at the start of the simulation and afterwards varies proportionally with changes in the number of dams. Gleick (2003) has projected future

damming pressure over the next 25 years by relating global water use to the number of new dams (Rosenberg et al., 2000). Based on this work, and the assumption that global water use is proportional to the world's population, we estimate that the number of dams should increase by 20% with an increase of the world's population by 1.9 billion people. Three damming scenarios are then considered, based on three projections for the change in the world population until the year 2100 (UN, 2005). The low, medium, and high damming scenarios are shown in Figure 4.

Additional effects of anthropogenic modifications of the earth surface environment are likely to affect Si cycling along the land-to-ocean continuum. On the time scales considered here (≤ 150 years), shifts in precipitation patterns and vegetation, changes in land-use and erosion will affect the cycling of Si on land and the delivery of reactive Si to the oceans (Conley et al., 2008). On even longer time scales, changes in thermohaline circulation accompanying a warming of the surface ocean will modify the exchanges of DSi between the surface and deeper parts of the oceans, thereby affecting marine biosiliceous productivity (see, e.g., Yool and Tyrell, 2005). A complete assessment of the response of the biogeochemical Si cycle to human-induced global change will thus require further work.

3. Results and Discussion

3.1 The global silica cycle

Most previous global scale mass balance studies of the Si cycle have focused on the oceans (Tréguer et al., 1995; De Master, 2002; Ragueneau et al., 2002; Yool and Tyrell, 2003, 2005; De La Rocha and Bickle, 2005). A novelty of the Si cycle presented here is that it includes an explicit representation of DSi and $bSiO_2$ cycling on the continents. Nevertheless, due to the relative scarcity of data, the estimates of the continental reservoir masses and fluxes have large uncertainties associated with them. For instance, the calculation of $bSiO_2$ stock in

soils assumes an average concentration of 5 mg phytoliths per g of soil. While the latter value is consistent with the $bSiO_2$ determinations in soils that have been made so far (Alexandre et al., 1997; Conley, 2002b; Clarke, 2003; Sferratore et al., 2006), it remains to be seen how representative the relatively limited set of existing measurements is for the global soil reservoir.

According to our estimates, phytoliths in soils and living terrestrial biomass constitute the largest fraction (65%) of the continental reactive Si reservoir. The amount of Si fixed by terrestrial and aquatic organisms on the continents on a yearly basis is estimated to be 89 Tmol y^{-1}. This value lies within the range of 60-209 Tmol y^{-1} given in the literature (Conley, 2002b) and is of the same order of magnitude as the rate of Si fixation in the oceans (244 Tmol y^{-1}). Thus, Si biomineralization on the continents is an important component of biological Si cycling on Earth (Conley, 2002a). As in the marine realm, siliceous productivity on the continents relies on the efficient regeneration of nutrient DSi through $bSiO_2$ dissolution. In our budget, 80% of the continental $bSiO_2$ produced is recycled, while the remainder accumulates in lacustrine sediments and in soils (Kendrick and Graham, 2004), or is exported to the oceans. Based on the estimates in Figure 2, the residence time of reactive Si on the continents is estimated to be 775 years.

Most reactive Si is delivered to the oceans by rivers under the form of DSi (F_{C1P1}; 6.2 Tmol y^{-1}). Nonetheless, the alternative supply routes of riverine $bSiO_2$ delivery ($F_{C4P2;}$ 1.1 ± 0.2 Tmol y^{-1}), submarine groundwater discharge ($F_{C1P1;}$ 0.4 ± 0.4 Tmol y^{-1}) and atmospheric transport ($F_{C2O2;}$ 0.5 ± 0.5 Tmol y^{-1}), together contribute about 25% of the transfer of reactive Si from the continents to the oceans. When hydrothermal inputs are also included ($F_{hyd;}$ 0.6 ± 0.4 Tmol y^{-1}), we estimate the total reactive Si delivery to the ocean to be 8.8 ± 1.5 Tmol y^{-1}. In comparison, Tréguer et al. (1995) estimated the total reactive Si supply to the oceans to be 6.7 ± 1.5 Tmol y^{-1}. These authors, however, did not account for the reactive Si input from

groundwater discharge and riverine $bSiO_2$. It should further be recognized that all regional sources of Si may not have been identified yet. For example, the venting of crustal fluids in the North Pacific has only recently been suggested to contribute as much as 1.5 ± 0.5 Tmol y^{-1} to the global oceanic Si budget (Johnson et al., 2006).

Assuming an initial steady-state, the sum of the inputs to the ocean is balanced by that of the outputs, and thus burial and reverse weathering should together yield a total removal flux of 8.8 Tmol y^{-1}. This value falls within the range for total reactive Si removal from the ocean of 8.4 to 9.4 Tmol y^{-1}, obtained when combining the estimated sediment burial fluxes of biogenic Si of DeMaster (2002; 7.4 - 8.4 Tmol y^{-1}) with that for reverse weathering (1.0 Tmol y^{-1}).

The explicit consideration of the proximal coastal zone enables us to account for the important filter function of estuaries, lagoons and embayments in nutrient cycles (Rabouille et al. 2001; Wollast, 1993; Seitzinger, 1996; Mackenzie et al., 2000). Significant Si processing decreases the $DSi/bSiO_2$ ratio from around 3 in rivers to 1.2 in the proximal zone. A net transformation of DSi into $bSiO_2$ is commonly observed in nearshore environments and causes a large fraction (43%, according to our model) of reactive Si to be delivered from the proximal to the distal coastal zone in the form of $bSiO_2$.

The fluxes in Figure 2 emphasize the role of the continental margins in removing reactive Si by sediment burial. Although the proximal and distal zones are only responsible for about 18% of the total biological fixation of DSi in the oceans, they may account for 40% of the total marine $bSiO_2$ burial, in line with the assessment of DeMaster (2002). The sum of the $bSiO_2$ burial fluxes in the proximal and distal coastal zones in our budget (3.1 Tmol y^{-1}) corresponds to the maximum of the range estimated by DeMaster (2002) for $bSiO_2$ burial along the continental margins (2.4 - 3.1 Tmol y^{-1}). It should be noted, however, that DeMaster's oceanic silica budget omits riverine supply of $bSiO_2$ and groundwater DSi

discharge. Our relatively high estimate for $bSiO_2$ accumulation in coastal sediments is consistent with the inclusion of these additional reactive Si inputs to the coastal zone, as well as the upward revision of the riverine DSi supply (6.2 versus 5.6 Tmol y^{-1}). The preferential burial of $bSiO_2$ in nearshore and shelf sediments is not only due to the relatively high sedimentation rates, but also to enhanced preservation resulting from interactions between deposited $bSiO_2$ and constituents solubilized from lithogenic minerals and the formation of new aluminosilicate phases (Van Cappellen et al., 2002; Dixit and Van Cappellen, 2003; Michalopoulos and Aller, 1995, 2004). In the proximal zone and especially in deltaic settings, there is a tight coupling between biogenic Si burial and reverse weathering, and analytical procedures for the measurement of biogenic silica account for reverse weathering products (Michalopoulos et al, 2000, Michalopoulos and Aller 1995, 2004:, Presti and Michalopoulos 2008). Thus, the Si burial flux used here for the proximal zone may include reverse weathering products.

The main inflow of DSi to the distal zone is caused by coastal upwelling, which is estimated to be on the order of 10 Tmol y^{-1} (Figure 2). The intermediate water masses of the open ocean (100-1000 m water depth) are assumed to be the source region for coastal upwelling. This assumption is consistent with mesopelagic DSi concentrations (25-30 μmol kg^{-1}; Dittmar and Birkicht, 2001; Brezinski et al., 1997), and Si/N ratios close to one (Hill and Wheeler, 2002; Brzezinski et al., 1997) reported for coastal upwelling waters. Deeper source regions (i.e., >1000 m) would yield higher DSi concentrations and Si/N ratios between 2 and 3 (Sverdrup et al., 1942).

Tréguer et al. (1995) estimated the whole-ocean residence time of reactive Si to be on the order of 15000 years. The latter value likely represents a lower limit, however, as these authors excluded the active surface layer of marine sediments in their calculation. According to the reservoir masses considered here, reactive Si in the water column and surface sediments

of the proximal coastal zone, distal coastal zone, plus the open ocean amounts to 149927 Tmol. The removal rate of reactive Si through burial and reverse weathering of 8.8 Tmol y^{-1} then implies a whole-ocean residence time of 17037 years. If the proximal coastal zone is excluded, the oceanic residence time of reactive Si is 20245 years. Estimated residence times for various marine reservoirs and their combinations are summarized in Table 4.

Interestingly, the residence times of reactive Si in the open ocean (10104 years) and the distal coastal zone (141 years) alone are significantly lower than the whole-ocean residence time (17037 years). This reflects the large exchange fluxes of reactive Si between the continental margins and the open ocean. For the distal zone in particular, these exchanges dominate the inputs and outputs of reactive Si and, hence, explain the relatively short residence time of reactive Si on the continental shelves.

Water column residence times of reactive Si are somewhat shorter than the corresponding water residence times (Table 4), because sinking of $bSiO_2$ by sedimentation decouples the Si cycle from the water cycle. Nonetheless, they are significantly lower than the values obtained when including sediments. The relative differences are particularly large for the proximal and distal coastal zone, because of the importance of benthic exchange fluxes of reactive Si. This is especially the case in the distal coastal zone, where benthic regeneration of silica accounts for nearly one-third of the reactive Si influx and is, therefore, a major source of reactive Si sustaining siliceous productivity in the overlying water column (Ragueneau et al., 2005).

3.2 Sensitivity analysis

To identify the most sensitive processes controlling Si cycling across the continent-ocean transition, we compute the relative changes in water column DSi and $bSiO_2$ concentrations of the coastal proximal and distal zones, induced by varying the rate constants

k_{ij} in the flux equations (Equation 2). In each simulation the value of one rate constant is increased by 50%, while all other model parameters remain unchanged. The sensitivity of the model to continental rock weathering (F_w) is similarly tested by increasing the value of F_w by 50%. Sensitivities are expressed as relative changes in DSi and $bSiO_2$ concentrations after 150 years of simulation time, relative to the initial, steady-state values.

The rate constants included in the sensitivity analysis correspond to the reactive Si fluxes that are not directly coupled to the water cycle via Equation (1). These fluxes include uptake and biomineralization of DSi, dissolution, sedimentation, and burial of $bSiO_2$, plus DSi efflux across the sediment-water interface. In addition, on the time scale considered (150 years), Si cycling in the proximal zone is not affected by processes occurring in the downstream distal coastal zone and open ocean reservoirs. Hence, the sensitivity analysis for the proximal zone is further limited to rate constants k_{ij} corresponding to processes occurring in the upstream, continental reservoir or within the proximal zone itself. In contrast, Si cycling in the distal coastal zone may also be affected by processes in the downstream open ocean reservoir, because of the return of oceanic waters onto the shelves via coastal upwelling.

The results of the sensitivity analysis are summarized in Table 5. DSi and $bSiO_2$ concentrations of proximal coastal waters are most sensitive to chemical weathering of continental rocks (F_w), terrestrial (F_{C1C2}), riverine (F_{C3C4}) and proximal coastal siliceous production (F_{P1P2}), and $bSiO_2$ dissolution on the continents (F_{C2C1}, F_{C4C3}, F_{C5C3}). Overall, enhanced production and sedimentation lead to lower DSi and $bSiO_2$ concentrations, while increased dissolution results in larger stocks of reactive Si in the water column. The main difference in the sensitivity of DSi and $bSiO_2$ concentrations in the proximal zone is related to the deposition of $bSiO_2$ in nearshore sediments (F_{P2P4}). While increasing k_{P2P4} causes a significant drop (-15%) of the $bSiO_2$ concentration in proximal waters, the DSi concentration is hardly affected. The latter reflects the fact that internal recycling of DSi via dissolution of

1 $bSiO_2$ within the proximal zone (F_{P2P1}, F_{P4P3}) is much less important than continental DSi
2 input (Figure 2). Thus, with the exception of nearshore siliceous production, reactive Si
3 dynamics in the proximal zone are primarily controlled by processes taking place on the
4 continents.

5 The sensitivity analysis reveals a different picture for the distal coastal zone (Table 5).
6 DSi and $bSiO_2$ concentrations in the distal coastal waters are most sensitive to internal
7 processes. These include DSi uptake and $bSiO_2$ dissolution in the water column (F_{S1S2}, F_{S2S1}),
8 as well as deposition (F_{S2S4}) and dissolution of $bSiO_2$ in the sediments (F_{S4S3}). Among the
9 sensitive upstream processes, those on the continents, especially terrestrial $bSiO_2$ production
10 and dissolution (F_{C1C2}, F_{C2C1}) and weathering (F_w), are more important than those in the
11 adjacent proximal coastal zone, although absolute changes larger than 4% are not observed.
12 Reactive Si cycling in the distal coastal zone is also sensitive to downstream processes,
13 foremost open ocean water column dissolution and sinking of $bSiO_2$ (F_{O4O3}, F_{O4O6}), as these
14 processes control the accumulation of DSi in the source waters of coastal upwelling.

15 On the time scale investigated, permanent removal of reactive Si through burial plays
16 a minor role in Si cycling at the Earth's surface. This contrasts with the dominant role of
17 sedimentary burial in the global biogeochemical Si cycle on geological time scales (De
18 Master, 2002; Van Cappellen, 2003). Nonetheless, even on the time scale of decades and
19 centuries, benthic-pelagic coupling is crucial to Si cycling in distal coastal waters (Conley,
20 1997; Ragueneau et al., 2002, 2005), as indicated by the high sensitivities to the deposition
21 (F_{S2S4}) and subsequent benthic dissolution of $bSiO_2$ (F_{S4S3}).

22 Changes in Si cycling at the land-ocean transition may also be caused by changes in
23 the water cycle. Nevertheless, reliable scenarios for the future evolution of the water cycle are
24 difficult to constrain. In addition to $bSiO_2$ retention, river damming causes a decrease of net
25 river flow to the oceans. In the proximal coastal zone, a reduction by 20% of the river

discharge (W_{1a2}) to the oceans results, after 150 years, in a relatively small decrease (4 %) in the concentration of DSi, but no change in that of $bSiO_2$. For the distal coastal zone, the corresponding changes are 3 and 4 % reductions in the concentrations of DSi and $bSiO_2$. The latter concentrations are further reduced (by 5 and 4 %, respectively) when the decrease in river discharge by 20% is accompanied by a 20% reduction in the coastal upwelling water flux (W_{43}). On longer time scales, changes in the water cycle (e.g., upwelling) may have significantly larger effects on global Si cycling (e.g., Yool and Tyrell, 2005).

3.3. Applications

3.3.1. Temperature rise

The three temperature scenarios yield the same general trends, but with different magnitudes (Figure 5). Except for open surface ocean DSi, increasing temperatures result in higher water column DSi and $bSiO_2$ concentrations. $bSiO_2$ concentrations in sediments of the continents and deep-sea are hardly affected, while they show opposite trends in the proximal (increase) and distal coastal ocean (decrease).

Rising concentrations of DSi and $bSiO_2$ in the continental aquatic environment (Box 1a, Figure 2) reflect enhanced DSi fluxes from weathering and $bSiO_2$ dissolution in soils. In combination with the relatively small volume of the aquatic environment, this causes significant, and parallel, increases in the DSi and $bSiO_2$ concentrations. Because of more rapid $bSiO_2$ dissolution kinetics, the additional reactive Si mobilized does not accumulate in sediments and soils, but is exported to the ocean.

Increased continental supply of reactive Si enhances siliceous productivity in proximal and distal coastal ecosystems. The largest relative change is observed in the $bSiO_2$ concentration of nearshore waters. That is, increased temperatures further decrease the water column DSi/$bSiO_2$ ratio of the proximal zone. The higher deposition flux of $bSiO_2$ offsets the

faster $bSiO_2$ dissolution kinetics, resulting in a net increase in the $bSiO_2$ concentration of proximal coastal sediments. Sediment $bSiO_2$ concentrations in the distal coastal zone show an opposite response, reflecting the very different recycling efficiencies of reactive Si in the two coastal systems (Figure 2). The latter is also reflected in the relative increases in water column DSi and $bSiO_2$ concentrations. In the proximal zone, rising temperatures cause a larger relative increase in $bSiO_2$, compared to DSi, while the reverse is observed for the distal zone. Possible indicators of a global warming effect on the Si cycle thus include opposite changes of water column DSi/$bSiO_2$ ratios and sediment $bSiO_2$ accumulation rates in proximal *versus* distal coastal environments.

Because of its much larger volume and of the buffering effect of the coastal zone, the open ocean exhibits much smaller modifications in Si cycling. The most pronounced changes are in the surface ocean, as it directly experiences changes in air temperature. Both DSi uptake and $bSiO_2$ dissolution rates are enhanced by rising temperature, resulting in faster Si turnover in the upper ocean. For the model structure and parameter values used here, the net effect is a slight increase in the $bSiO_2$ standing stock, at the expense of the DSi pool.

3.3.2. River damming

River damming leads to opposite trends of DSi and $bSiO_2$ concentrations compared to those of temperature rise, with the exception of $bSiO_2$ in distal coastal sediments (Figure 5, broken lines). Predicted concentration changes also imply that damming should increase water column DSi/$bSiO_2$ ratios in continental aquatic systems and the proximal coastal zone. A number of studies have indeed reported measurable increases in DSi/$bSiO_2$ ratios of riverine and nearshore waters (Conley 1997, 2002b; Friedl and Wuest, 2002).

As expected, the sedimentary $bSiO_2$ pool on the continents increases as biosiliceous debris accumulates behind the growing number of dams. The decreased continental supply of

reactive Si causes a relative drop in sediment $bSiO_2$ in nearshore marine sediments and an increase on the continents. It should be borne in mind, however, that the reservoir size of proximal coastal zone sediment $bSiO_2$ (110 Tmol Si) is much smaller than that of continental sediments (1417 Tmol Si). At the scale investigated in our simulations, damming causes more $bSiO_2$ to be trapped in continental sediments than lost from proximal sediments.

A general feature of the response of Si cycling to changes in damming is the "dilution" of the relative effects from rivers to the open ocean (Figure 5). Typically, the largest changes in reactive Si concentrations are observed in aquatic systems on land and in the proximal coastal zone, while the open ocean system experiences little changes. For example, the open ocean surface DSi concentration is predicted to change by less than 1% after 150 years, even for the highest damming scenario.

According to the damming scenarios, the largest increase in the number of dams should have taken place between the 1950s and the present. After 2000, the different damming scenarios hypothesize the same decreasing damming pressure until 2025, after which the three scenarios diverge (Figure 4). The time-dependent features imposed to the damming scenarios are recorded nearly instantaneously by the water column DSi and $bSiO_2$ concentrations in the continental aquatic system and the proximal coastal zone, because of the correspondingly very short residence times of reactive Si (2.1 and 0.7 years, Table 4). This is not the case for the sediment $bSiO_2$ concentrations in the same reservoirs. Because of much longer residence, and hence response times, the initial trends (i.e., for the period 1950-2000) are projected into the future with still little differentiation in sediment $bSiO_2$ concentrations among the scenarios by the year 2050.

3.3.3. Combined river damming and temperature rise

A set of nine permutations of the three temperature and three damming scenarios were run. The results are illustrated in Figure 6 for the intermediate temperature rise plus maximum damming scenario. This particular scenario was selected because it exhibits the main features observed in all the various simulations. The comparison between Figures 5 and 6 suggests that river damming is driving the changes in Si cycling in the combined scenario, particularly during the initial period (1950-2000). On the continents, the results of the combined simulation closely follow those of the damming-only simulation, except for the slight rise in water column DSi concentration simulated beyond 2050. The slowing down of dam construction after 2000 and continued rise in temperature cause much more pronounced reversals in the water column DSi concentrations of the coastal ocean. By the end of the simulation, the DSi concentration in the proximal zone has returned to within 2% of its starting value, while in the distal zone the DSi concentration increases above the initial value.

The water column $bSiO_2$ concentration in the proximal coastal zone mainly records the changing damming pressure. This is no longer the case for the distal coastal zone, since reactive Si cycling in this reservoir is largely driven by internal recycling, via temperature-dependent DSi uptake and $bSiO_2$ dissolution. Thus, as far as the water column DSi and $bSiO_2$ concentrations are concerned, when moving from the continents to the open ocean, the relative influence of changes in river damming decreases, while that of global warming increases.

Changes in sediment $bSiO_2$ concentrations in the combined scenario are essentially the same as in the damming-only scenario, for all reservoirs. The lack of temperature-induced changes reflects the much longer residence times of reactive Si in the sediment reservoirs, relative to the water column. That is, over the 150 years of simulation time, the sediments only record the initial rapid growth in the number of dams after the 1950s. The observed loss

of sediment $bSiO_2$ in coastal environments over the simulation period is therefore mainly due to reactive Si retention by dams.

The results presented in Figures 5 and 6 illustrate the complex response of Si cycling to human influences. In particular, the temporal trends in DSi and $bSiO_2$ concentrations in the combined damming plus temperature rise scenario are not simply the sum of the individual responses to the two perturbations. Nonetheless, the results also indicate that by combining temporal trends in DSi and $bSiO_2$ concentrations in multiple reservoirs it may become possible to extricate the relative effects of the different anthropogenic forcings acting on the biogeochemical Si cycle.

4. Conclusions

Silicon is a key nutrient whose biogeochemical cycling is closely coupled to those of carbon, nitrogen, phosphorus, iron and trace compounds. Large amounts of dissolved Si (DSi) are biologically fixed annually as biogenic silica ($bSiO_2$), both on land (89 Tmol y^{-1}) and in the oceans (240 Tmol y^{-1}). The estimated residence time of reactive Si on the continents (775 years), however, is about 20 times smaller than for the oceans (17037 years), reflecting the much larger marine reservoir of reactive Si.

While reactive Si is mainly exported from the continents as riverine DSi (6.2 Tmol y^{-1}), a non-negligible fraction is delivered to the oceans as $bSiO_2$ in river suspended matter and in eolian dust deposits (1.6 Tmol y^{-1}), and as DSi in submarine groundwater discharge (0.4 Tmol y^{-1}). Because of the net transformation of DSi into $bSiO_2$ in nearshore waters, nearly half (43%) of land-derived reactive Si reaching the distal coastal zone is in the form of $bSiO_2$. Nevertheless, the major input of reactive Si to the continental shelves is via coastal upwelling.

The coastal ocean represents a dynamic interface between the continents and the open ocean. Although coastal and shelf environments account for only 18% of all biological Si fixation in the oceans, an estimated 40% of all marine $bSiO_2$ burial takes place in nearshore

and shelf sediments (3.2 Tmol y^{-1}). Nearshore ecosystems also attenuate the downstream propagation of land-based perturbations of the Si cycle that results from damming of rivers or land-use changes.

The biogeochemical Si cycle is currently undergoing significant modifications due to human activities. The proposed model can help delineate the expected changes, through sensitivity analyses and scenario simulations. A major difficulty is that multiple anthropogenic perturbations are simultaneously acting on the Si cycle. The results presented here, and observed changes in rivers and nearshore waters, indicate that riverine export of reactive Si, and the riverine $bSiO_2$/DSi ratio, are likely to continue to drop in the near future, as a result of reactive Si retention by dams. However, enhanced $bSiO_2$ dissolution due to global warming may ultimately allow coastal siliceous productivity to recover from the downward trend caused by river damming.

Our work represents a first step towards modeling the global biogeochemical Si cycle along the entire land to ocean continuum. Further progress will rely especially on the increased understanding and characterization of the spatial heterogeneity of continental Si cycling, caused by differences in lithology, vegetation, land-use and hydrology. This information is needed to account for the regional variability in reactive Si delivery to the coastal zone by rivers and submarine groundwater discharge.

Acknowledgements

This project was initiated during the 2004 Summer School of the EU-funded Research Training Network SiWEBS (contract number HPRN-CT-2002-000218). Further work on the project was made possible by financial support from the EU (SiWEBS), Utrecht University (High Potential project G-NUX to C.P. Slomp) and the Netherlands Organisation for

Scientific Research (NWO Pioneer grant to P. Van Cappellen). We thank the editor and the anonymous reviewers for their useful and constructive comments.

References

Alexandre, A., J.-D. Meunier, F. Colin and J. M. Koud (1997) Plant impact on the biogeochemical cycle of silicon and related weathering processes. *Geochim. Cosmochim. Acta, 61*, 677-682.

Alvarez-Salgado, X.A., C.G. Castro, F.F. Pérez and F. Fraga (1997) Nutrient mineralization patterns in shelf waters of the Western Iberian upwelling, Continental Shelf Research 17, 1247–1270.

Anikouchine, W.A and R.W. Sternberg (1981) *The World Ocean: An Introduction to Oceanography*, Prentice-Hall, NJ, USA.

Appelo, C. A. J. and D. Postma (1993) *Geochemistry, Groundwater and Pollution*, Balkema, Amsterdam.

Arhondistis, G. E. and M. T. Brett (2005) Eutrophication model for Lake Washington (USA) Part II—model calibration and system dynamics analysis. *Ecological Modelling*, 187, 179-200.

Batjes, N.H. (1997) A world data set of derived soil properties by FAO UNESCO soil unit for global modeling, Soil Use Manage. 13, 9–16.

Bartoli, F. (1983) The biogeochemical cycle of silicon in two temperateforest ecosystems. *Ecological Bulletin 35*, 469–476.

Berelson, W. M., D. E. Hammond and K. S. Johnson (1987) Benthic fluxes and the cycling of biogenic silica and carbon in the two southern California Borderland Basins. *Geochim. Cosmochim. Acta*, *51*, 1345–1363.

Berner, E. A. and R. A. Berner (1996) *Global Environment: Water, Air and Geochemical Cycles* Prentice-Hall.

Biscaye, P. E., C. N. Flagg and P. G. Falkowski (1994) The shelf edge exchange processes experiment, SEEP-II: an introduction to hypotheses, results and conclusions. *Deep-Sea Res. II*, *41*, 231-252.

Blum, A.E. and L.L. Stillings (1995) Feldspar dissolution kinetics, in *Chemical Weathering Rates of Silicate Minerals* edited by A.E. White and S.L. Brantley, pp. 291-351. Mineralogical Society of America.

Bonn, W.J. (1995) Biogenic opal and barium: Indicators for late Quarternary changes in productivity at the Antarctic continental margin, Atlantic Sector. *Reports on Polar Research*, *180*, 186pp., Alfred Wegener Institute for Polar and Marine Research, Bremerhaven.

Brink, K. H., F. F. G. Abrantes, P. A. Bernal, R. C. Dugdale, M. Estrada, L. Hutchings, R. A. Jahnke, P. J. Muller and R. L. Smith (1995) Group report: How do coastal upwelling systems operate as integrated physical, chemical, and biological systems and influence the geological record?, in *Upwelling in the Ocean: Modern Processes and Ancient Records* edited by C. P. Summerhayes, K.-C. Emeis, M. V. Angel, R. L. Smith and B. Zeitzeschel, pp. 103–124.

Broecker, W.S. and T.-H. Peng (1982) *Tracers in the Sea.* A publication of the L-D geological Observatory. Columbia University, Palisades, New York. Eldigio Press.

Brzezinski, M.A., D. R. Phillips, F. P. Chavez, G. E. Friederich and R. C. Dugdale (1997) Silica production in the Monterey, California, upwelling system. *Limnol. Oceanogr.*, *42*, 1694-1705.

Chauvaud, L., F. Jean, O. Ragueneau and G. Thouzeau (2000) Long-term variation of the Bay of Brest ecosystem: benthic–pelagic coupling revisited. *Mar. Ecol. Prog. Series*, *200*, 35–48.

Chameides, W. L. and E. M. Perdue (1997) *Biogeochemical Cycles. A Computer-Interactive Study of Earth System Science & Global Change. Oxford University Press*, New York / Oxford, 1997

Clarke, J. (2003) The occurrence and significance of biogenic opal in the regolith, *Earth Sci Rev., 60*, 175-194.

Cole, J. M., Goldstein, S. L., deMenocal, P. B., Hemming, S. R. and F. E. Grousset (2009) Contrasting compositions of Saharan dust in the eastern Atlantic Ocean during the last deglaciation and African Humid Period. *Earth and Planetary Science Letters*, 278, 257–266.

Conkright, M., S. Levitus and T. P. Boyer (1994) NOAA Atlas NESDIS 1. World Ocean Atlas 1994, *Nutrients*, vol. 1, U.S. Government Printing Office, Washington, D.C., USA.

Conley, D. J. (1988) Biogenic silica as an estimate of siliceous microfossil abundance in Great-Lakes sediments. *Biogeochemistry*, *6*(3), 161-179.

Conley, D. J. (1997) Riverine contribution of biogenic silica to the oceanic silica budget. *Limnol. Oceanogr.*, *42*, 774-777.

Conley, D. J. (2002a) The biogeochemical silica cycle: Elemental to global scales. *Océanis*, *28*, 353-368.

Conley, D. J. (2002b) Terrestrial ecosystems and the global biogeochemical silica cycle. *Global Biogeochem. Cycle*, *16*, 1121, doi: 10.1029/2002GB001894.

Conley D.J., Kilham, S.S. and E. Theriot (1989) Differences in silica content between marine and freshwater diatoms. *Limnol. Oceanogr.* 34, 205-213.

Conley, D. J., C.L. Schelske, and E.F. Stoermer (1993) Modification of the biogeochemical cycle of silica with eutrophication. *Mar. Ecol. Prog. Series*, *101*, 179-192.

Conley, D. J., P. Stålnacke, H. Pitkänen, and A. Wilander (2000) The transport and retention of dissolved silicate from rivers in Sweden and Finland. *Limnol. Oceanogr.*, 45, 1850-1853.

Conley, D. J. and T. C. Malone (1992) Annual cycle of dissolved silicate in Chesapeake Bay-implications for the production and fate of phytoplankton biomass. *Mar. Ecol. Prog. Series*, *81*, 121–128.

Conley D. J. and C. L. Schelske (2001) Biogenic silica. in: *Tracking Environmental Changes Using Lake Sediments: Biological Methods and Indicators*, edited by J. P. Smol, H. J. B. Birks and W. M. Last, pp. 281-293. Kluwer Academic Press, Dordrecht.

Conley D. J., G. E. Likens, D. Buso, L. Saccone, S. W. Bailey, and C. Johnson (2008) Deforestation causes increased dissolved silicate losses in the Hubbard Brook Experimental Forest. *Global Change Biol.* 14, 2548-2554.

Cossins, A.R. and K. Bowler (1987) Temperature biology of animals. Chapman and Hall, New York, New York.

Datnoff, L. E., G. H. Snyder and G. H. Korndörfer (2001) *Silicon in agriculture*, edited by L. E. Datnoff, , G. H. Snyder and G. H. Korndörfer, Elsevier Sci., Amsterdam.

Del Amo, Y. and M.A. Brzezinski (1999) The chemical form of dissolved Si taken up by marine diatoms. *Journal of Phycology, 35 (6),* 1162-1170.

De La Rocha, C. L. and M. J. Bikle (2005) Sensitivity of silicon isotopes to whole-ocean changes in the silica cycle, *Mar. Geol.*, *217*, 267–282.

DeMaster, D.J., (2002) The accumulation and cycling of biogenic silica in the Southern Ocean: revisiting the marine silica budget. *Deep-Sea Res. II*, *49*, 3155-3167.

Dittmar, T. and M. Birkicht (2001) Regeneration of nutrients in the northern Benguela upwelling and the Angola-Benguela Front areas, *South African Journal of Science*, *97*(5-6), 239-246.

Dixit, S. and P. Van Cappellen, (2003) Predicting benthic fluxes of silicic acid from deep-sea sediments. *J. Geophys. Res.*, *108*(C10), 3334, doi:10.1029/2002JC001309.

Dürr H.H., Meybeck M., Hartmann J., Laruelle G.G., Roubeix V. (submitted). Global spatial distribution of natural riverine silica inputs to the coastal zone. *under review in Biogeosciences Discussions*

Egge, J.K. and D.L. Aksnes (1992) Silicate as a regulating nutrient in phytoplankton competition. *Mar. Ecol. Prog. Series*, *83*, 281-189.

Eppley, R. W. (1972) Temperature and phytoplankton growth in the sea. *Fishery Bull.*, *70*, 1063-1085.

Epstein, E. (1999) Silicon. *Ann. Rev. Plant Physiol. Plant Molec. Biol.*, *50*, 641-664.

Fekete, B.M., Vörösmarty, C.J. and W. Grabs (2002). High-resolution fields of global runoff combining observed river discharge and simulated water balances. *Global Biogeochemical Cycles*, *16*(3), 1042, doi:10.1029/1999GB001254.

Food and Agriculture Organization/U.N. Educational, Scientific and Cultural Organization (FAO/UNESCO), (1986). Gridded FAO/UNESCO soil units: UNEP/GRID, FAO soil map of the world in digital form, digital raster data on 2-minute geographic (lat x lon) 5400 x 10800 grid, Carouge, Switzerland.

Friedl, G. and A. Wüest, (2002) Disrupting biogeochemical cycles – Consequences of damming.*Aquatic Science*, *64*, 55-65.

Friedl, G., C. Teodoru and B. Wehrli (2004) Is the Iron Gate I reservoir on the Danube River a sink for dissolved silica? *Biogeochemistry*, *68*, 21-32.

Garnier, J., A. D'Ayguesvives, J. Billen, D. J. Conley and A. Sferratore (2002) Silica dynamics in the hydrographic network of the Seine River. *Océanis*, *28*, 487-508.

Garrels, R. M. and F. T. Mackenzie (1971) *Evolution of Sedimentary Rocks,* edited by W.W. Norton, 397pp., New York.

Gerard, F. and J. Ranger (2002) Silicate weathering mechanisms in a forest soil. *Océanis*, *28*, 384-415.

Gibson, C.E., B.M. Stewart and R.J. Gowen (1997) A synoptic study of nutrients in the north–west Irish Sea, Estuarine, Coastal and Shelf Science 45, 27–38.

Gleick, P.H. (2003) Global freshwater resources: Soft-path solutions for the 21st Century. *Science*, *302*,1524-1528.

Heinze, C., E. Maier-Reimer, A. M. E. Winguth and D. Archer (1999) A global oceanic sediment model for long-term climate studies, *J. Geophys. Res*., *13*(1), pp. 221, doi:98GB02812.

Heiskanen, A.S. and A. Keck (1996) Distribution and sinking rates of phytoplankton, detritus, and particulate biogenic silica in the Laptev Sea and Lena River (Arctic Siberia), Mar. Chem. 53, 229–245.

Hill, J.K. and P. A. Wheeler (2002) Organic carbon and nitrogen in the northern California current system: comparison of offshore, river plume and coastally upwelled water. *Progress in Oceanography*, *53*, 369-387.

Humborg, C., D. J. Conley, L. Rahm, F. Wulff, A. Cociasu and V. Ittekot (2000) Silicon retention in river basins: far-reaching effects on biogeochemistry and aquatic food webs in coastal marine environments. *Ambio*, *29*(1), 45–51.

Humborg, C., M. Pastuszak, J. Aigars, H. Siegmund, C. M. Morth, V. Ittekkot (2006) Decreased silica land-sea fluxes through damming in the Baltic Sea catchment - Significance of particle trapping and hydrological alterations. *Biogeochemistry 77*(2), 265-281.

Jahnke, R. A., S. R. Emerson and J. W. Murray (1982) A model of oxygen reduction, denitrification, and organic matter mineralization in marine sediments. *Limnol. Oceanogr.*, *27*, 610-630.

Johnson, H. P., S. L. Hautala, T. A. Bjorklund, and M. R. Zarnetske (2006) Quantifying the North Pacific silica plume. *Geochem., Geophys., Geosys*. 7: doi:10.1029/2005GC001065.

Kendrick, K. J. and R. C. Graham. (2004) Pedogenic silica accumulation in chronosequence soils, Southern California. *Soil Sci. Soc. Amer. J. 68,* 1295-1303.

Koning, E., G,-J. Brummer, W. Van Raaphorst, J. Van Bennekom, W. Helder and J. Van Ipperen (1997) Settling, dissolution and burial of biogenic silica in the sediments off Somalia (northwestern Indian Ocean). *Deep-Sea Res. II*, *44*, 1341–1360.

Lacroix, G., Ruddick, K., Park, Y., Gypens, N. and C. Lancelot (2007). Validation of the 3D biogeochemical model MIRO&CO with field nutrient and phytoplankton data and MERIS-derived surface chlorophyll a images. *Journal of Marine Systems* 64 (1–4), 66–88.

Lasaga, A. C. (1981) Rate laws of chemical reactions, in *Kinetics of Geochemical Processes*, Vol. 8, edited by Lasaga, A. C. and R. J. Kirkpatrick, pp. 1–169. Mineralogical Society of America.

Lasaga, A.C. (1998) *Kinetic Theory in the Earth Sciences.* Princeton, New Jersey: Princeton University Press.

Ledford-Hoffman, P. A., D. J. DeMaster and C. A. Nittrouer (1986) Biogenic silica accumulation in the Ross Sea and the importance of Antarctic continental-shelf deposits in the marine silica budget. *Geochim. Cosmochim. Acta*, *50*, 2099-2110.

Levitus, S.J.L., T.P. Antonov, Boyer, and C. Stephens, (2000) Warming of the world ocean. *Science*, *287*., 2225 – 2229.

Leynaert, A., P. Tréguer, and C. Lancelot (2001) Silicic acid limitation of Equatorial Pacific diatom populations : evidence from ^{32}Si kinetic experiments. *Deep-Sea Res.*, *48*, 639-660.

Macdonald, A. M. (1998) The global ocean circulation: a hydrographic estimate and regional analysis. *Progress in Oceanography*, *41*, 281–382.

Mackenzie, F. T. and R.A. Garrels (1966) Chemical mass balance between rivers and oceans. *Amer. J. Sci.*, *264*, 507-525.

Mackenzie, F. T., A. Lerman, and L. M. Ver (1998) Role of the continental margin in the global carbon balance during the past three centuries. *Geology*, *26*, 423–426.

Mackenzie, F. T., L. M. Ver and A. Lerman (2000) Coastal-zone biogeochemical dynamics under global warming. *Int. Geol. Rev.*, *42*, 193–206.

Mackenzie, F. T., L. M. Ver, C. Sabine, M. Lane and A. Lerman (1993) C, N, P, S global biogeochemical cycles and modeling of global change. in *Interactions of C, N, P and S Biogeochemical Cycles and Global Change*, edited by Wollast, R., F. T. Mackenzie and L. Chou, pp.1–62. Springer-Verlag.

Maher, K., DePaolo D. J. and Lin J. C.-F. (2004) Rates of silicate dissolution in deep-sea sediment: in situ measurement using 234U/238U of pore fluids. *Geochim. Cosmochim. Acta*, *68*(22), 4629-4648.

Meunier, J.D., F. Colin, C. Alarcon (1999) Biogenic silica storage in soils. *Geology, 27* (9), 835-838.

Meybeck M, L. Laroche, H. H. Dürr and J. P. M. Syvitski (2003) Global variability of daily total suspended solids and their fluxes in rivers. *Global and Planetary Change, 39* (1-2), 65-93

Meybeck, M. and A. Ragu (1995), River discharges to oceans: An assessment of suspended solids, major ions and nutrients, report, *U.N. Environ. Programme*, Nairobi.

Michalopoulos, P. and R. C. Aller (1995) Rapid clay mineral formation in Amazon delta sediments: reverse weathering and oceanic elemental fluxes. *Science*, *270*, 614–617.

Michalopoulos, P and R.C. Aller (2004) Early diagenesis of biogenic silica in the Amazon delta: alteration, authigenic clay formation, and storage, *Geochim. Cosmochim. Acta, 68*, 1061–1085.

Michalopoulos P., Aller R. C., and Reeder R. J. (2000) Conversion of diatoms to clays during early diagenesis in tropical, continental shelf muds. *Geology, 28*, 1095–1098.

Nelson, D.M., P. Tréguer, M. A. Brzezinski, A. Leynaert and B. Queguiner (1995) Production and dissolution of biogenic silica in the ocean: revised global estimates, comparison with regional data and relationship to biogenic sedimentation. *Global Biogeochem. Cycles*, *9*, 359–372.

Paasche, E. (1980) Silicon. in *The Physiological Ecology of Phytoplankton*, edited by Morris, I., pp. 259-284. Blackwell Scientific Publications, Oxford.

Pasquer, B., G. Laurelle, S. Bequevort, V. Schoemann, H. Goosse and C. Lancelot (2005) Linking ocean biochemical cycles and ecosystem structure and function: results of the complex SWAMCO model, *J. Sea Res.*, *53*, 93–108.

Piperno D. R. (1988) *Phytolyth analysis – an archeological and geological perspective*. pp. 280, Academic Press, London.

Pouba, Z. (1968). Geologische Kartierung (czech.). NAKLAD. Ceskoslowenske, Akademii Ved, Prague.

Presti, M., and P. Michalopoulos. (2008) Estimating the contribution of the authigenic mineral component to the long-term reactive silica accumulation on the western shelf of the Mississippi River Delta. *Continental Shelf Research, 28*, 823-838.

Rabouille, C., F.T. Mackenzie, and L.M. Ver (2001) Influence of the human perturbation on carbon, nitrogen, and oxygen biogeochemical cycles in the global coastal ocean. *Geochim. Cosmochim. Acta*, *65*(21), 3615-3641.

Rabouille, C., P. Crassous, A. Kripounoff, J.-F. Gaillard, R. Jahnke, C. Pierre and J.-C. Relexans. (1993) A model of early diagenesis in the tropical North Atlantic: Processes and mass balances in the sediments of the EUMELI program, *Chemical Geology*, *107*, 463-466.

Ragueneau, O., Dittert, N., Corrin, L., Tréguer, P. and P. Pondaven (2002). Si:C decoupling in the world ocean: is the Southern Ocean different ? *Deep-Sea Research II, 49 (16)*, 3127-3154.

Ragueneau, O., Chauvaud, L., Moriceau, B., Leynaert, A., Thouzeau, G., Donval, A., Le Loc'h, F. and F. Jean (2005) Biodeposition by an invasive suspension feeder impacts the biogeochemical cycle of Si in a coastal ecosystem (Bay of Brest, France). *Biogeochemistry, DOI 10.1007/s10533-004-5677-3*.

Ragueneau, O., S. Schultes, K. Bidle, P. Claquin, and B. Moriceau (2006a) Si and C Interactions in the world ocean: Importance of ecological processes and implications for the role of diatoms in the biological pump, *Global Biogeochemical Cycles, 20*, GB4S02, doi:10.1029/2006GB002688.

Ragueneau, O., D. J. Conley, S. Ni Longphuirt, C. P. Slomp, A. Leynaert (2006b) A review of the Si biogeochemical cycle in coastal waters, I. Diatoms in coastal food webs and the coastal Si cycle. in: *Land-ocean nutrient fluxes: silica cycle*, edited by Ittekot, V., C. Humborg and J. Garnier. SCOPE, in press.

Ragueneau, O., D.J. Conley, S. Ni Longphuirt, C.P. Slomp, A. Leynaert. (2006c) A review of the Si biogeochemical cycle in coastal waters, II. Anthropogenic perturbation of the Si cycle and responses of coastal ecosystems. in: *Land-ocean nutrient fluxes: silica cycle*, edited by Ittekot, V., C. Humborg and J. Garnier. SCOPE, in press.

Rao, A. M. F. and R. A. Jahnke (2004) Quantifying porewater exchange across the sediment-water interface in the deep sea with in situ tracer studies, *Limnol. Oceanogr.: Methods*, *2*, 75–90.

Rickert, D. (2000) Dissolution kinetics of biogenic silica in marine environments. in : *Reports on Polar Research*, vol. 351, pp. 211., Alfred Wegener Institute for Polar and Marine Research.

Rosenberg, D. M., P. McCully, and C. M. Pringle. (2000) Global-scale environmental effects of hydrological alterations: introduction. *BioScience, 50*,746-751.

Saccone, L., D. J. Conley, G. E. Likens, S. W. Bailey, D. C. Buso, and C.E. Johnson (2008) Distribution of amorphous silica in soils of the Hubbard Brook Experimental Forest. *Soil Sci. Soc. J. Amer.* 72, 1637-1644.

Seitzinger, S.P. and A.E. Giblin. (1996) Estimating denitrification in North Atlantic continental shelf sediments. *Biogeochemistry, 35*, 235-259.

Serebrennikova, Y.M. and K.A. Fanning (2004) Nutirents in the Southern Ocean GLOBEC region: variations, water circulation, and cycling, Deep-Sea Research, Part II 51, 1981–2002.

Schroeder, D. (1978). *Bodenkunde in Stichworten*. Verlag Ferdinand Hirt, 154 pp

Simpson, T.L. and B. E. Volcani (1981) *Silicon and siliceous structures in biological systems*. Springer-Verlag, New York.

Sferratore, A., J. Garnier, G. Billen, D. Conley, and S. Pinault (2006). Silica diffuse and point sources in the Seine watershed. *Environmental Science & Technology*, *40*: 6630-6635.

Slomp, C. P. and P. Van Cappellen (2004) Nutrient inputs to the coastal ocean through submarine groundwater discharge: Controls and potential impact, *J. Hydrol.*, *295*, 64-86.

Sverdrup, H. V., M. W. Johnson and R. H. Fleming (1942) *The Oceans*. Englewood Cliffs, N. J., Prentice-Hall.

Tréguer, P., D. M. Nelson, A. J. Van Bennekom, D. J. DeMaster, A. Leynaert, and B. Queguiner (1995) The silica balance in the world ocean: A reestimate, *Science New Series*, *268*(5209), 375-379.

Van Cappellen, P., S. Dixit and J. Van Beusekom (2002) Biogenic silica dissolution in the oceans: reconciling experimental and field-based dissolution rates. *Global Biogeochem. Cycles*, *16*(4),1075, doi:10.1029/2001GB001431.

Van Cappellen, P. (2003) Biomineralization and global biogeochemical cycles. in: *Biomineralization* edited by Dove, P., J. DeYoreo and S. Weiner, pp. 357-381, Reviews in Mineralogy and Geochemistry, 54, Mineral. Soc. Amer., Washington, D. C.

Ver, L. M. (1998) Global kinetic models of the coupled C, N, P, and S biogeochemical cycles: Implications for global environmental change. Ph.D. dissertation, University of Hawaii.

Winkler, J. P., R. S. Cherry and W. H. Schlesinger (1996) The Q10 relationship of microbial respiration in a temperate forest soil. *Soil Biol. Biochem.*, *28*, 1067–1072.

Wollast, R. (1974) The silica problem. in: The Sea edited by Goldberg E. D. pp. 359-392, Wiley.

Wollast, R. (1991) The coastal organic carbon cycle: Fluxes, sources, and sinks. in: *Ocean Margin Processes in Global Change*, edited by Mantoura, R. F. C., J. M. Martin, and R. Wollast, pp. 365–381. Wiley-Interscience.

Wollast, R. (1993) Interactions of carbon and nitrogen cycles in the coastal zone. in : *Interactions of C, N, P and S Biogeochemical Cycles and Global Change*, edited by. Wollast, R., F. T. Mackenzie, and L. Chou, pp. 195–210, Springer-Verlag.

Woodwell, G. M., Rich P. H., and Hall C. A. S. (1973) Carbon in estuaries. in Carbon and the Biosphere. edited by Woodwell G. M. and E. V. Pecan, pp. 221–240. U.S. Atomic Energy Commission, CONF-720510.

Yool, A. and T. Tyrrell (2003) The role of diatoms in regulating the ocean's silicon cycle. *Glob. Biogeochem. Cycles*, *17*, 1103, doi:10.1029/2002GB002018.

Yool, A. and T. Tyrrell (2005) Implications for the history of Cenozoic opal deposition from a quantitative model. *Palaeogeography, Palaeoclimatology, Palaeoecology*, *218*, 239–255.

Zhang, J. (2002) Biogeochemistry of Chinese estuarine and coastal waters: nutrients, trace metals and biomarkers. *Reg. Environ. Change, 3*, 65-76.

Table 1. Calculations and references used to constrain the water fluxes in the model.

Flux	Value ($Tm^3\ y^{-1}$)	Calculation	Reference
$W_{1b\text{-}1a}$	39	-	(1)
$W_{1a\text{-}2}$	39	$W_{4a\text{-}1} - W_{1b\text{-}2}$	-
$W_{1b\text{-}2}$	2	-	(2)
$W_{2\text{-}3}$	41	$W_{1a\text{-}2} + W_{1b\text{-}2}$	-
$W_{3\text{-}4}$	441	$W_{2\text{-}3} - W_{4\text{-}3}$	-
$W_{4\text{-}3}$	400	-	(3,4,5)
$W_{4a\text{-}4b}$	3800	$W_{4b\text{-}4a} + W_{3\text{-}4} - W_{4a\text{-}1}$	-
$W_{4b\text{-}4a}$	3400	-	(6)
$W_{4b\text{-}4c}$	472	-	(6)
$W_{4c\text{-}4b}$	472	$W_{4b\text{-}4c}$	-
$W_{4a\text{-}1b}$	41	-	(7)

(1) Fekete et al., 2002; (2) Slomp and Van Cappellen, 2004; (3) Brink et al., 1995; (4) Ver, 1998 ; (5) Rabouille et al., 2001 ; (6) Deduced from residence time in Broecker and Peng, 1982; (7) Anikouchine and Sternberg (1981);

Table 2. Reservoir sizes of dissolved silicate (DSi) and biogenic silica ($bSiO_2$) in the model. V(x) and VS(x) refer to the volu

box x as described in Figure 1. The porosity (ϕ = 0.7) and the density (ρ = 2.5 g cm^{-3}) of the sediments are taken from Mahe

for the atomic mass of Si and molar weight of SiO_2 respectively.

	Reservoir	Size (Tmol Si)	Calculation
Continents			
C1	Terrestrial DSi	3060	200 µmol Si L^{-1} [(a)] × V(1b) [(b)]
			a- average DSi concentration in ground waters
			b- volume of ground waters
C2	Terrestrial $bSiO_2$	8250	0.42g Si^{-1} [(a)] × 0.005 g g^{-1} [(b)] × (75.10^{18} m^2 [(c)] × 1m [(d)] × 2.65 g.cm
			a- mass of Si per gram of phytoliths
			b- average mass of phytoliths per gram of soil
			c- global surface area covered by soils
			d- assumed global average soil depth
			e- average dry density of soils
			f- solid fraction of soils
C3	Aquatic $bSiO_2$	3.6	-
C4	Aquatic DSi	20.5	(9.3 mg Si L^{-1} [(a)] × V(1b) [(b)])/M(Si)
			a- average DSi concentration in rivers
			b- global volume of lakes and floodplains
C5	$bSiO_2$ in river and lake sediments	1416	50 mg SiO_2 g sediment $^{-1}$ [(a)] / M(SiO_2) × VS(1) [(b)] × (1- ϕ) × ρ
			a- average $bSiO_2$ content of river sediments
			b- volume of lake plus river sediments
Proximal Coastal Zone			
P1	DSi in the water column	3.2	F_{P1S1} × V(2)/W_{2-3}
P2	$bSiO_2$ in the water column	2.4	F_{P2S2} × V(2)/W_{2-3}
P3	pore water DSi in sediments	0.2	300 µmol Si L^{-1} × VS(2) × ϕ
P4	$bSiO_2$ in sediments	110	0.02 g Si g^{-1} [(a)] × VS(2) × (1- ϕ) × ρ /M(Si)
			a- mass of Si as $bSiO_2$ in proximal coastal sediments (2 wt%)

Table 2 *(continued)*

	Reservoir	Size (Tmol Si)	Calculation
Distal Coastal Zone			
S1	DSi in the water column	72	F_{S1O1} x V(3) / $W_{3\text{-}4a}$
S2	$bSiO_2$ in the water column	32	F_{S2O2} x V(3) / $W_{3\text{-}4a}$
S3	pore water DSi in sediments	1	300 µmol Si L^{-1} × VS(3) × ϕ
S4	$bSiO_2$ in sediments	2190	0.03 g Si $g^{-1\,(a)}$ × VS(3) × (1- ϕ) × ρ / M(Si)
			a- mass of Si as $bSiO_2$ in distal coastal sediments (3 wt%)
Open Ocean			
O1	DSi in the surface ocean	187	5 µmol L^{-1} × V(4a)
O2	$bSiO_2$ in the surface ocean	37	1 µmol L^{-1} × V(4a)
O3	DSi in intermediate waters	8438	25 µmol L^{-1} × V(4b)
O4	$bSiO_2$ in intermediate waters	170	0.5 µmol L^{-1} × V(4b)
O5	DSi in deep sea	87750	100 µmol L^{-1} × V(4c)
O6	$bSiO_2$ in deep sea	290	0.1 µmol L^{-1} × V(4c)
O7	pore water DSi in sediments	17	300 µmol Si L^{-1} × VS(4) × ϕ
O8	$bSiO_2$ in sediments	50625	0.05 g Si $g^{-1\,(a)}$ × VS(4) × (1- ϕ) × ρ / M(Si)
			a- mass of Si as $bSiO_2$ in deep sea sediments (5 wt%)

Sources : (1) J.-D. Meunier, comm. pers. ; (2) Berner and Berner, 1996 ; (3) Conley, 2002b ; (4) FAO/UNESCO soil map of

(6) Conley, 1997 ; (7) Dürr et al., submitted ; (8) Conley, 1988 ; (9) Jahnke et al., 1982; (10) Ledford-Hoffman et al., 1986

Tyrell, 2003; (13) Conkright et al., 1994 ; (14) Dittmar and Birkicht, 2001 ; (15) Hill and Wheeler, 200

Table 3. Silicon fluxes in the model. V and VS refer to the volumes of water and sediment reservoirs, respectively, Si/C is the molar ratio of the exported organic matter, M(Si) and M(C) stand for the atomic mass of Si and C respectively.

	Flux	Flux (Tmol y^{-1})	Calculation or explanation
Continents			
F_w	*Weathering*	14.6	$F_{C1C2} - F_{C2C1} + F_{C1C3} + F_{C1P1}$
$F_{C2\text{-}burial}$	*Terrestrial $bSiO_2$ burial*	3.6	25% of F_w
F_{C1C2}	*Terrestrial DSi uptake*	80	reported range: 60 to 200 Tmol Si y^{-1}
F_{C1C3}	*DSi export from box 1b to box 1a*	7.8	
F_{C1P1}	*DSi export from box 1b to box 2*	0.4	$W_{1b\text{-}2}$ x 200 µmol Si L^{-1} in ground waters
F_{C2C1}	*Terrestrial $bSiO_2$ dissolution*	73.6	92% of F_{C1C2}
F_{C2O2}	*Eolian silica export*	0.5	
F_{C2C4}	*$bSiO_2$ export to rivers*	2.3	
F_{C3C4}	*DSi uptake in rivers*	9.3	61%[(a)] of carbon primary production × 17.10^{12} m^2 [(b)] × 13.5g C a- fraction of primary production due to diatoms in fresh water b- surface of rivers and lakes c- Average riverine primary production in carbon d- molar Si to C ratio of 0.79±0.43
F_{C3P1}	*DSi export from box 1a*	6.2	
F_{C4C3}	*$bSiO_2$ dissolution*	6.3	
F_{C4C5}	*$bSiO_2$ Sedimentation in rivers*	4.2	$F_{C2C4} + F_{C3C4} - F_{C4P1} - F_{C4C3}$
F_{C4P2}	*$bSiO_2$ export from box 1a*	1.1	
F_{C5C3}	*Sediment $bSiO_2$ dissolution*	1.4	
$F_{C5\text{-}burial}$	*Aquatic $bSiO_2$ burial*	2.8	$F_{C4C5} - F_{C5C3}$
Proximal Coastal Zone			
F_{P1P2}	*DSi uptake*	4.5	75% [(a)] of carbon primary production (40 Tmol C y^{-1} [(b)]) × (Si/C a- fraction of primary production due to diatoms in the coastal b- primary production in the proximal coastal zone in carbon c- molar Si to C ratio of 0.15
F_{P1S1}	*DSi export from box 2*	3.6	$P1 \times W_{2\text{-}3}$
F_{P2P1}	*$bSiO_2$ dissolution*	0.9	$F_{P1P2} + F_{C4P2} - F_{P2S2} - F_{P2P4}$
F_{P2P4}	*Sedimentation*	2	$F_{P4P3} + F_{P4\text{-}burial}$
F_{P2S2}	*$bSiO_2$ export from box 2*	2.7	$F_{P1P2} - F_{P2P4} - F_{P2P1}$
F_{P3P1}	*DSi efflux*	0.6	Within the range of 0.8 ± 0.4 Tmol Si y^{-1} given by 3.6 Tm^2 × 2
F_{P4P3}	*Sediment $bSiO_2$ dissolution*	0.6	F_{P3P1}
$F_{P4\text{-}burial}$	*$bSiO_2$ Burial*	1.4	$P4 \times 0.13$ cm y^{-1} [(a)]/ 10 cm [(b)] (and so that $F_{P4\text{-}burial} + F_{S4\text{-}burial}$ a- sediment accumulation rate in the proximal coastal zone b- depth of the active sediment layer in the proximal coastal zo

Table 3 *(continued)*

	Flux	Flux (Tmol y^{-1})	Calculation or explanation
Distal Coastal Zone			
F_{S1S2}	*DSi uptake*	40	[18% [(a)] of global siliceous primary production (240 Tmol Si y a- fraction of the global marine primary production occurring i b- estimate of the global marine siliceous production
F_{S2S1}	*$bSiO_2$ dissolution*	31	
F_{S1O1}	*$bSiO_2$ export from box3*	9.6	$F_{S2S1} + F_{S3S1} + F_{O3S1} + F_{P1S1} - F_{S1S2}$
F_{S2S1}	*$bSiO_2$ dissolution*	31	$F_{S1S2} + F_{P2S2} - F_{S2S4} - F_{S2O2}$
F_{S2S4}	*Sedimentation*	7.7	$F_{S4\text{-}burial} + F_{S4S3}$
F_{S2O2}	*$bSiO_2$ export from box3*	4	assuming the same export rate as organic carbon, 10% of F_{S1S2}
F_{S3S1}	*DSi efflux*	5	within the range of 6 ± 3 Tmol Si y^{-1} given by 27 $Tm^{2(a)}$ × 0.2 a- surface area of the distal coastal zone b- estimate of benthic efflux rate for the continental shelf
$F_{S3\text{-}rw}$	*Reverse weathering*	1	
F_{S4S3}	*$bSiO_2$ dissolution*	6	$F_{S3\text{-}rw} + F_{S3S1}$
$F_{S4\text{-}burial}$	*$bSiO_2$ Burial*	1.7	$S4 \times 0.016$ cm y^{-1} [(a)] / 20 cm [(b)] (so that $F_{P4\text{-}burial} + F_{S4\text{-}burial} = 3$ a- sediment accumulation rate in the proximal coastal zone b- depth of the active sediment layer in the proximal coastal zc
Open Ocean			
F_{O1O2}	*DSi uptake*	200	240 Tmol Si $y^{-1} - F_{S1S2}$
F_{O2O1}	*$bSiO_2$ dissolution*	104.9	within the range of 100 – 120 Tmol Si y^{-1} (50 [(a)] to 60 [(b)] % of a- fraction of $bSiO_2$ production preserved in the water column b- fraction of $bSiO_2$ production preserved in the water column
F_{O2O4}	*Sedimentation*	99.1	$F_{O1O2} + F_{atm} - F_{O2O4}$
F_{O3S1}	*Coastal upwelling*	10	$[O_3 / V(4b)] \times W_{4\text{-}3}$
F_{O3O1}	*Oceanic upwelling*	85	$F_{O4O3} + F_{O5O3} - F_{O3S1}$
F_{O4O3}	*$bSiO_2$ dissolution*	52.5	($F_{O6O5} + F_{O4O3}$ = 38% of F_{O1O2} [(1)])
F_{O4O6}	*Sedimentation*	46.6	$F_{O2O4} - F_{O4O3}$
F_{O5O3}	*Deep upwelling*	42.5	$F_{O6O5} + F_{O7O5}$
F_{O6O5}	*$bSiO_2$ dissolution*	22.6	($F_{O6O5} + F_{O4O3}$ = 38% of F_{O1O2} [(1)])
F_{O6O8}	*Sedimentation*	24	12% of F_{O1O2}
F_{O7O5}	*DSi efflux*	19.9	within the range of 23 ± 15 Tmol Si y^{-1}
F_{O8O7}	*Sediment $bSiO_2$ dissolution*	19.3	$F_{O7O5} - F_{hyd}$
$F_{O8\text{-}burial}$	*$bSiO_2$ burial*	4.7	within the range of 4.1-4.3 Tmol Si y^{-1} [(a)] and 6 Tmol Si y^{-1} [(b)] a- estimate of $bSiO_2$ preservation in marine sediments b- assuming 3% preservation of opal in marine sediments
F_{hyd}	*Hydrothermal input*	0.6	

(1) Alexandre et al., 1997; (2) Conley, 2002b; (3) Appelo and Postma, 1996 ; (4) Tréguer et al., 1995; (5) Arhonditsis a

1996 ; (7) Garnier et al., 2002 ; (8) Conley et al., 1989 ; (9) Dürr et al., submitted ; (10) Nelson et al., 1995 ; (11) Ra

1987 ; (13) De Master, 2002 ; (14) Heinz et al., 1999 ;(15) Biscaye et al., 1994 ; (16) Wollast, 1991 ; (17) M

Formatted: English U.K.

Table 4. Reactive silica contents and residence times in the various compartments of the earth surfa

	DSi + bSiO$_2$ (Tmol Si)	*Export + Burial (Tmol Si y^{-1})*	*Residence time (y)*	*U*
Continents (box1)				
Terrestrial	11310	14.6	775	0.
Rivers and Lakes	24.1	10.1	2.1	5.
River and Lakes + Sediment	1441.1	10.1	143	-
Proximal Coastal Zone (box 2)				
Water Column	5.6	7.7	0.7	0.
Water Column + Sediment	115.6	7.7	15	-
Distal Coastal Zone (box 3)				
Water Column	104	16.3	4.9	2.
Water Column + Sediment	2295	16.3	141	-
Open Ocean (box 4)				
Water Column	96875	14.6	6635	1
Water Column + Sediment	147517	14.6	10104	-
World Ocean (box 2+3+4)				
Water Column	96984.6	8.8	11021	2
Water Column + Sediment	149927.8	8.8	17037	-

Table 5. Sensitivity analysis: % change in DSi and $bSiO_2$ concentrations in proximal (Box 2) and distal coastal zone (Box3) 150 years after increasing the corresponding flux or rate constant by 50%.

Modified parameter	Type of process	% DSi in box 2	% $bSiO_2$ in box 2	% DSi in box 3	% $bSiO_2$ in box 3
Fw	Weathering	7	6	2	2
k_{C1C2}	Uptake	-13	-11	-3	-4
k_{C2C1}	Dissolution	14	12	3	4
k_{C3C4}	Uptake	-15	-9	-3	-4
k_{C4C3}	Dissolution	13	8	3	3
k_{C4C5}	Sedimentation	-10	-13	-3	-4
$k_{C5\text{-}burial}$	Burial	-1	-1	0	0
k_{C5C3}	Dissolution	5	5	1	1
k_{P1P2}	Uptake	-21	15	-2	-1
k_{P2P1}	Dissolution	5	-4	0	0
k_{P2P4}	Sedimentation	0	-15	-2	-2
k_{P3P1}	Efflux	0	0	0	0
$k_{P4\text{-}burial}$	Burial	-2	-2	-1	-1
k_{P4P3}	Dissolution	3	3	1	1
k_{S1S2}	Uptake	-	-	-25	11
k_{S2S1}	Dissolution	-	-	21	-10
k_{S2S4}	Sedimentation	-	-	-9	-17
$k_{S3\text{-}rw}$	Reverse weathering	-	-	-2	-2
k_{S3S1}	Efflux	-	-	2	2
$k_{S4\text{-}burial}$	Burial	-	-	-1	-1
k_{S4S3}	Dissolution	-	-	10	9
k_{O1O2}	Uptake	-	-	0	0
k_{O2O1}	Dissolution	-	-	0	0
k_{O4O3}	Dissolution	-	-	1	1
k_{O6O5}	Dissolution	-	-	0	0
k_{O6O8}	Sedimentation	-	-	0	0
k_{O7O5}	Efflux	-	-	0	0
$k_{O8\text{-}burial}$	Burial	-	-	0	0
k_{O8O7}	Dissolution	-	-	0	0

Figure Captions

Figure 1. Global Water Cycle with water masses in Tm^3 and water fluxes (W) in $Tm^3\ y^{-1}$. V = volume and τ = residence time.

Figure 2. Steady state biogeochemical cycle of silicon, with reservoirs in Tmol Si and fluxes in Tmol Si y^{-1}. Shaded squares represent $bSiO_2$ reservoirs, open squares represent DSi reservoirs. The steady state cycle of Si is used as initial condition (nominally 1950) in the perturbation simulations.

Figure 3. Temperature scenarios for surface and intermediate waters used as forcing functions in the simulations.

Figure 4. River damming scenarios used in the simulations. The three curves represent the relative change in damming pressure, relative to 1950, for low, medium and high damming scenarios.

Figure 5: Relative changes in DSi (top), water column $bSiO_2$ (middle) and sediment $bSiO_2$ (bottom) reservoir sizes versus time for the three different temperature (continuous lines), and damming (dashed lines) scenarios. In black, the high temperature or damming scenario, in gray the medium temperature or damming scenario, and in light gray the low temperature or damming scenario.

Figure 6: Relative changes in DSi (top), water column $bSiO_2$ (middle) and sediment $bSiO_2$ (bottom) reservoir sizes versus time for the combined scenario with high damming and medium temperature forcing.

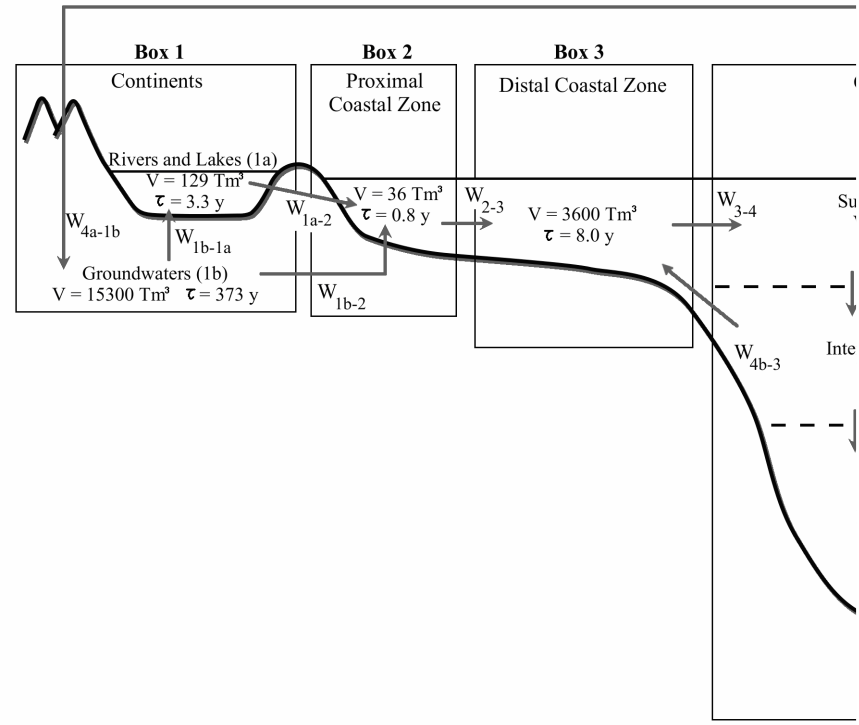
Box 1
Continents
Box 2
Proximal
Coastal Zone
Box 3
Distal Coastal Zone
Rivers and Lakes (1a)
V = 129 Tm³
τ = 3.3 y
W4a-1b
W1b-1a
W1a-2
V = 36 Tm³
τ = 0.8 y
W2-3
V = 3600 Tm³
τ = 8.0 y
W3-4
Groundwaters (1b)
V = 15300 Tm³ τ = 373 y
W1b-2
W4b-3

Figure 1.

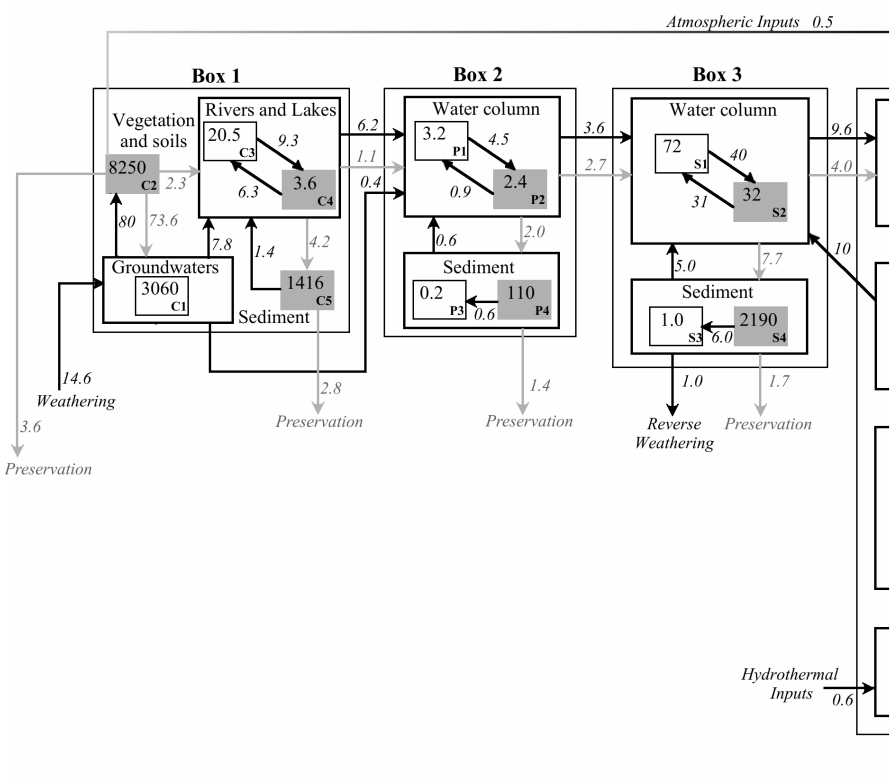
Atmospheric Inputs 0.5
Box 1
Box 2
Box 3
Vegetation and soils
8250
C2
2.3
Rivers and Lakes
20.5
C3
9.3
6.3
3.6
C4
6.2
1.1
0.4
Water column
3.2
P1
4.5
0.9
2.4
P2
3.6
2.7
Water column
72
S1
40
31
32
S2
9.6
4.0
10
80
73.6
7.8
1.4
4.2
Groundwaters
3060
C1
1416
C5
Sediment
0.6
2.0
Sediment
0.2
P3
0.6
110
P4
5.0
7.7
Sediment
1.0
S3
6.0
2190
S4
14.6
Weathering
3.6
Preservation
2.8
Preservation
1.4
Preservation
1.0
Reverse Weathering
1.7
Preservation
Hydrothermal Inputs
0.6

Figure 2.

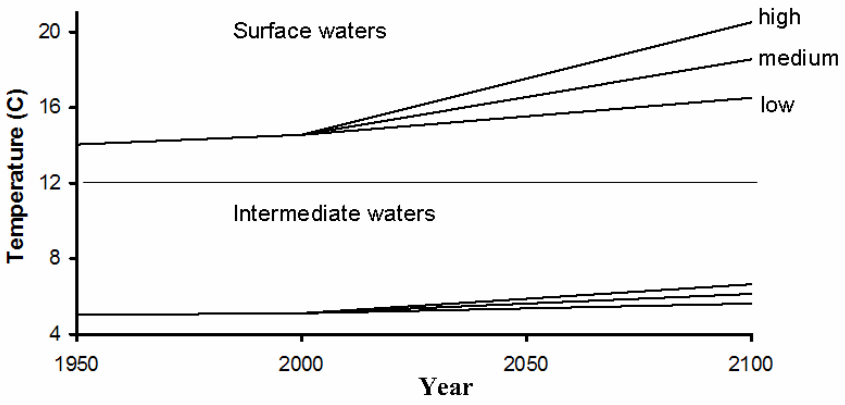
Surface waters
high
medium
low
Intermediate waters
Temperature (C)
20
16
12
8
4
1950
2000
2050
2100
Year

Figure 3.

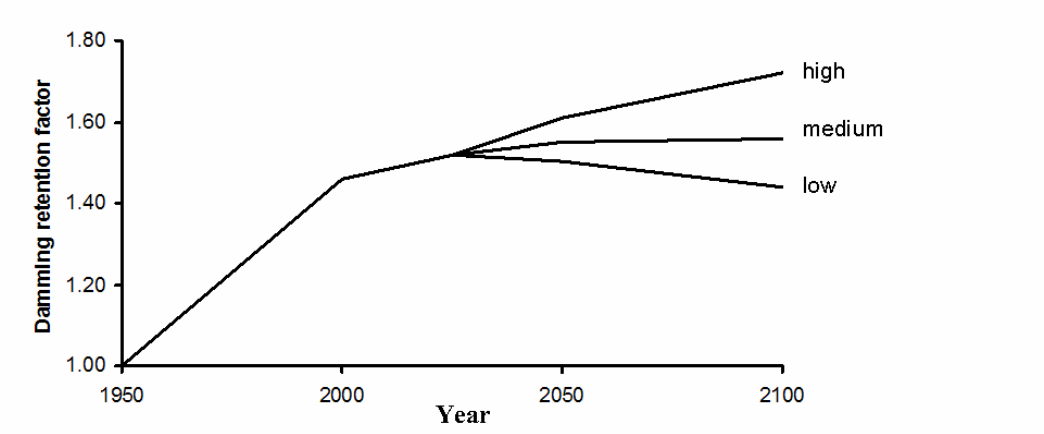
1.80
1.60
1.40
1.20
1.00
Dammlng retention factor
high
medium
low
1950
2000
2050
2100
Year

Figure 4.

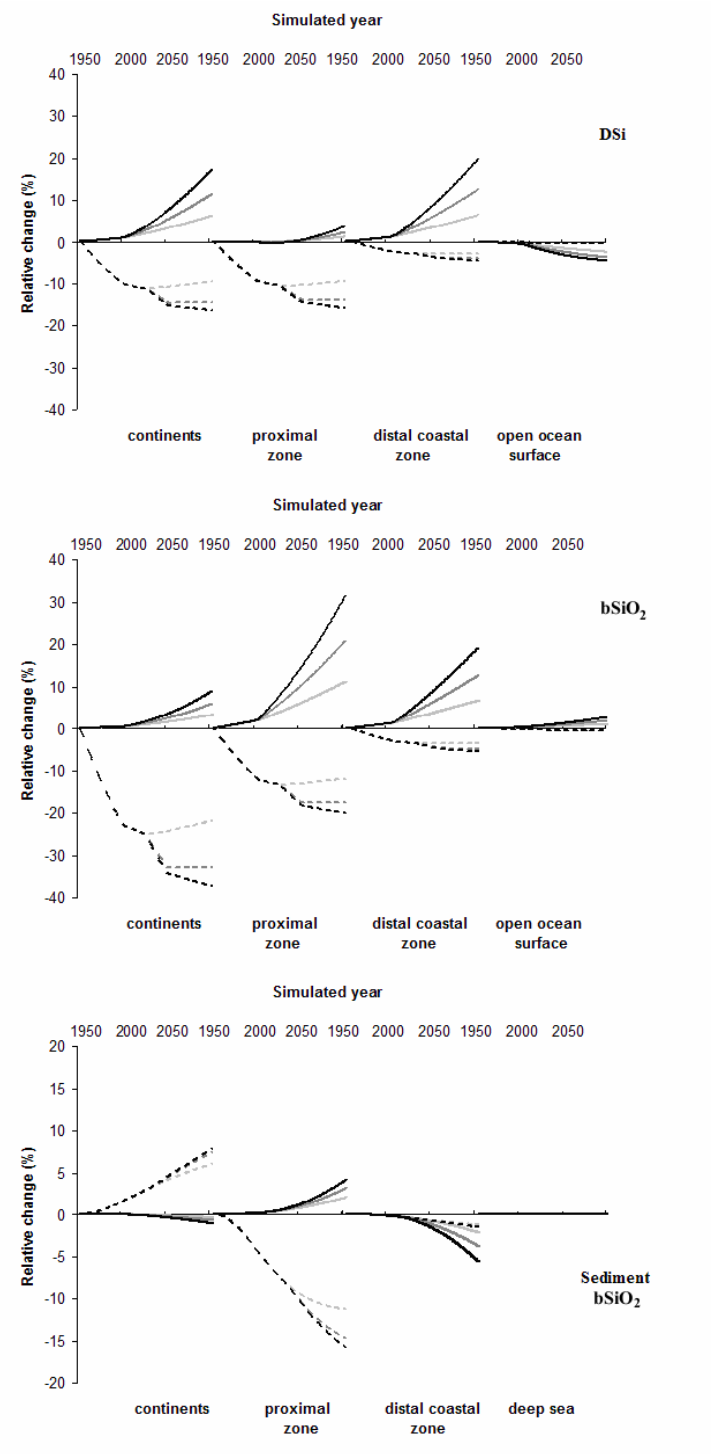
Simulated year
1950 2000 2050 1950 2000 2050 1950 2000 2050 1950 2000 2050
DSi
Relative change (%)
40 30 20 10 0 -10 -20 -30 -40
continents
proximal zone
distal coastal zone
open ocean surface
Simulated year
1950 2000 2050 1950 2000 2050 1950 2000 2050 1950 2000 2050
bSiO2
Relative change (%)
40 30 20 10 0 -10 -20 -30 -40
continents
proximal zone
distal coastal zone
open ocean surface
Simulated year
1950 2000 2050 1950 2000 2050 1950 2000 2050 1950 2000 2050
Sediment bSiO2
Relative change (%)
20 15 10 5 0 -5 -10 -15 -20
continents
proximal zone
distal coastal zone
deep sea

Figure 5.

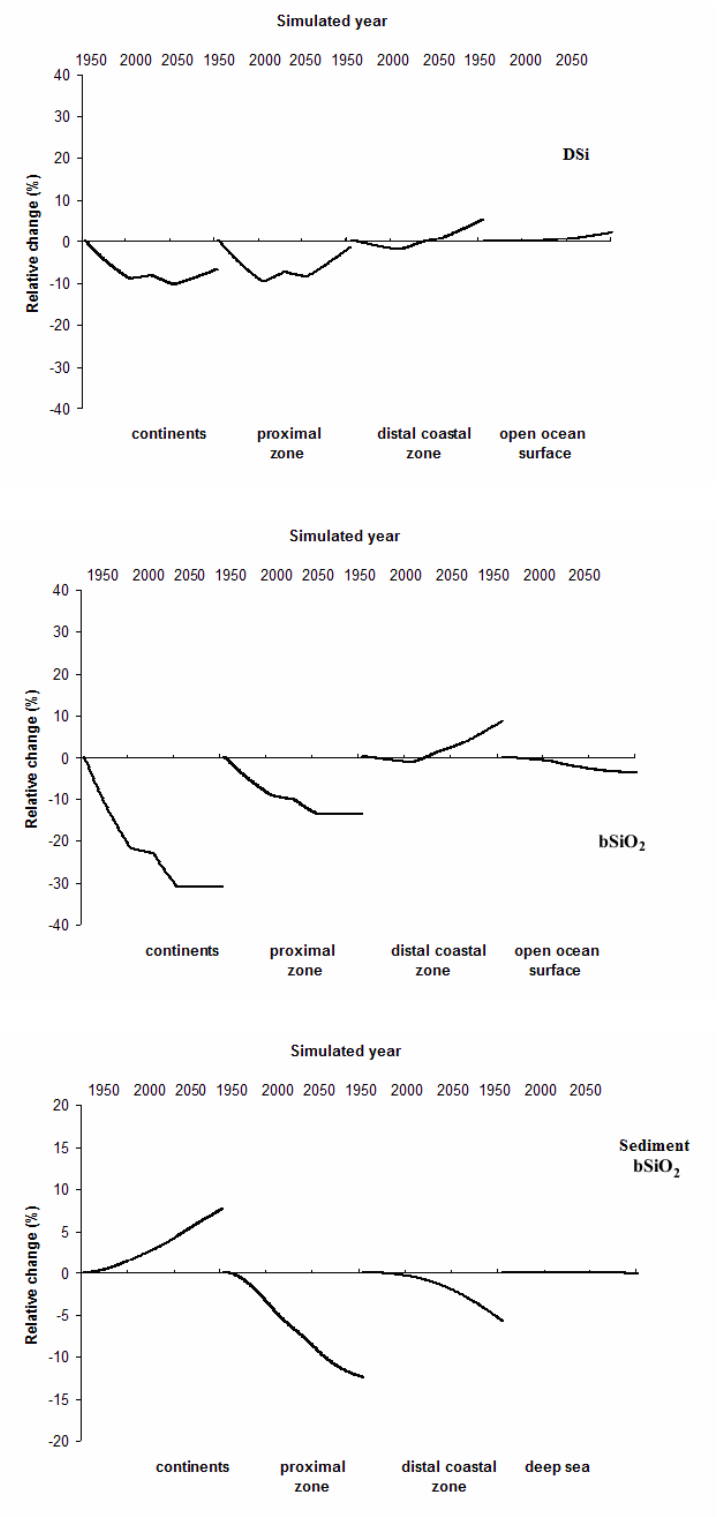
Simulated year
1950 2000 2050 1950 2000 2050 1950 2000 2050 1950 2000 2050
Relative change (%)
40
30
20
10
0
-10
-20
-30
-40
DSi
continents
proximal zone
distal coastal zone
open ocean surface
Simulated year
1950 2000 2050 1950 2000 2050 1950 2000 2050 1950 2000 2050
Relative change (%)
40
30
20
10
0
-10
-20
-30
-40
bSiO2
continents
proximal zone
distal coastal zone
open ocean surface
Simulated year
1950 2000 2050 1950 2000 2050 1950 2000 2050 1950 2000 2050
Relative change (%)
20
15
10
5
0
-5
-10
-15
-20
Sediment bSiO2
continents
proximal zone
distal coastal zone
deep sea

Figure 6.